

## MODE-LOCKED ERBIUM-DOPED FIBER LASER WITH TITANIUM DIOXIDE SATURABLE ABSORBER

Z. S. SALLEH<sup>a</sup>, E. I. ISMAIL<sup>a</sup>, N. A. KADIR<sup>a</sup>, A. A. LATIFF<sup>b</sup>, M. YASIN<sup>c</sup>, Z. JUSOH<sup>a</sup>, S. W. HARUN<sup>a,b,\*</sup>, H. AROF<sup>a</sup>

<sup>a</sup>*Department of Electrical Engineering, University of Malaya, 50603 Kuala Lumpur, Malaysia*

<sup>b</sup>*Photonics Research Centre, University of Malaya, 50603 Kuala Lumpur, Malaysia*

<sup>c</sup>*Department of Physics, Faculty of Science and Technology, Airlangga University, Surabaya (60115) Indonesia*

<sup>d</sup>*Faculty of Electrical Engineering, Universiti Teknologi Mara (Terengganu), 23000 Dungun, Terengganu, Malaysia*

We demonstrate a stable mode-locked Erbium-doped fiber laser (EDFL) by employing a titanium dioxide (TiO<sub>2</sub>) polymer composite film as a passive SA. The film has a loss of 3.0 dB and modulation depth of 40.0% at 1550 nm. A 186 m long single-mode fiber (SMF) is added into the laser cavity so that it operates in normal dispersion regime. The ring laser produces a stable dissipative soliton mode-locking pulse as the input pump power is maintained within 73 mW to the maximum power of 157 mW. The laser has a central wavelength, 3 dB spectral bandwidth, pulse duration, and repetition rate of 1563 nm, 0.39 nm, 271.3 ns, and 1.038 MHz, respectively. The maximum pulse energy of 6.25 nJ is obtained at the maximum input pump power of 157 mW. This result suggests that TiO<sub>2</sub> could be further investigated for pulsed laser applications.

(Received August 27, 2016; Accepted October 31, 2016)

*Keywords:* Titanium dioxide (TiO<sub>2</sub>) polymer composite film, Passive saturable absorber, Mode-locking

### 1. Introduction

Ultra-short pulse fiber lasers have gained increasing interest due to their great potential applications in fields such as spectroscopy, fiber communication and biomedical diagnoses [1-2]. Up to now, most of these lasers have adopted passive mode-locking technique, in which saturable absorbers (SAs) act as a key component. The improvement of lasers relies on the optical properties of SAs, for instance, transparency and optical non-linearity. There have been attempts on several types of SAs materials. Semiconductor SA mirrors (SESAMs) currently dominate passive mode-locking. However, some intrinsic disadvantages of SESAMs still remain, such as limited operation bandwidth and complex fabrication/packaging [3]. Therefore, many works are devoted to two dimensional (2D) nanomaterials, such as graphene [4-5], topological insulator (TI) [6] and molybdenum disulfide (MoS<sub>2</sub>) [7] for generating ultrafast fiber lasers. This is mainly attributed to their remarkable advantages such as ultrafast recovery time, controllable modulation depth, and saturable absorption characteristics.

Recently, titanium (IV) dioxide (TiO<sub>2</sub>), a newly emerging semiconductor nanomaterial, has also gained wide attention in recent years as a thin film material for potential application in microelectronic layered structures [8]. Some important parameters that determine the Q-switching and mode-locking abilities of a saturable absorber are recovery time, absorption characteristic, modulation depth and damage threshold. TiO<sub>2</sub> has a recovery time of ~1.5 ps when observed using 780 nm, 250-fs laser [9]. An open-aperture Z-scan on TiO<sub>2</sub> films also reveals nonlinear optical

---

\*Corresponding author: swharun@um.edu.my

properties known as saturable absorption and two-photon absorption [10]. Although the band gap of TiO<sub>2</sub> is ~3.2 eV (387 nm) [11], its spectral absorption can be extended until the near-infrared (NIR) region [12]. This can be explained by the quantum size effect of TiO<sub>2</sub>, where the absorption depends on the crystal form and particle size [13].

Herein, we demonstrate a passive mode-locked fiber laser utilizing a free-standing TiO<sub>2</sub>/polyvinyl alcohol (PVA) nanocomposite film as a mode-locker. PVA is used because of its capability to form film while having favorable physical properties such as good chemical resistance, biocompatibility and hydrophilicity [14].

## 2. Preparation and characterization of the TiO<sub>2</sub> based SA

We prepare TiO<sub>2</sub> solution by solving commercially available anatase TiO<sub>2</sub> powder in distilled water with the assistance of 1% sodium dodecyl sulphate (SDS) solvent. The TiO<sub>2</sub> powder is 99% pure and has a diameter of less than 45 μm. The mixture was then stirred for 5 minutes so that the TiO<sub>2</sub> material was dispersed homogeneously. The TiO<sub>2</sub> solution was centrifuged at speed of 3000 rpm for 15 minutes and the supernatant containing the TiO<sub>2</sub> suspension in solution was collected for use. The dispersed TiO<sub>2</sub> solution was then added into a polymer solution of 1 g PVA powder in 120 ml deionized water (DI). The mixture was stirred at 90°C until the polymer was completely dispersed. It is then cooled down to room temperature. Then the TiO<sub>2</sub> and PVA mixture was thoroughly mixed through a centrifuging process to form a composite precursor solution. Finally the precursor solution was poured onto a glass petri dish and heated in a vacuum oven for nearly 2 days to form a free standing film.

Raman spectroscopy was then performed by exciting the fabricated film sample by a 514 nm laser to verify the presence of TiO<sub>2</sub> material. The Raman spectrum obtained is shown in Fig. 1. It exhibits five distinct Raman peaks at approximately 145, 198, 399, 516, and 640 cm<sup>-1</sup>, which correspond to the first E<sub>g</sub>, second E<sub>g</sub>, B<sub>1g</sub>, A<sub>1g</sub>, and third E<sub>g</sub> band, respectively. The result is in good agreement with the Raman spectrum reported by Balachandran & Eror [15]. The high peak intensity at 145 cm<sup>-1</sup> confirms that this TiO<sub>2</sub> is only observed in the Raman spectrum of anatase crystalline structure.

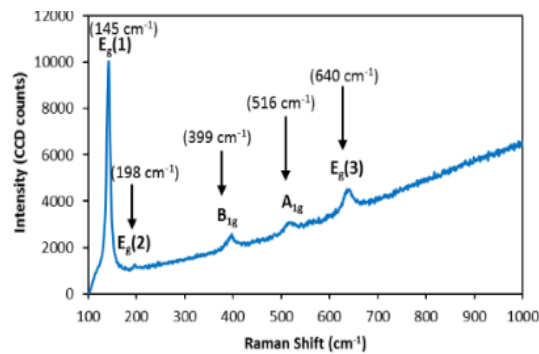


Fig. 1: Raman spectrum of the fabricated TiO<sub>2</sub> film.

Twin detector measurement technique was then employed to characterize the nonlinear optical response of this fabricated TiO<sub>2</sub> film sample. In the experiment, a stable self-constructed passively mode-locked fibre laser operating at 1560 nm with a frequency repetition rate of 26 MHz and pulse duration of 600 fs was used as the input pulse light source. The output powers from both detectors were recorded as we gradually increased the output power value. From the result, the absorption was calculated and later, was fitted using the following saturation model formula [16]:

$$\alpha(I) = \frac{\alpha_s}{1 + I/I_{sat}} + \alpha_{ns}$$

where  $\alpha(I)$  is the absorption rate,  $\alpha_s$  is the modulation depth,  $I$  is the input light intensity,  $I_{sat}$  is the saturation intensity, and  $\alpha_{ns}$  is the non-saturable absorption. The absorptions at various input intensities were recorded and plotted as shown in Fig. 2 after curve fitting using the above saturation model formula. The saturation intensity and modulation depth of the saturable absorber are  $0.008 \text{ MW/cm}^2$  and  $40.0 \%$ , respectively. The saturation intensity for different saturable absorber are  $58.59 \text{ MW/cm}^2$  for  $\text{Bi}_2\text{Te}_3$  [17] and  $0.43 \text{ MW/cm}^2$  for  $\text{MoS}_2$  [18]. Taking into account its nonlinear optical response may lead to absorption saturation at relatively low fluence, the  $\text{TiO}_2$  film is expected to function very well as a passive SA in a fiber laser setup.

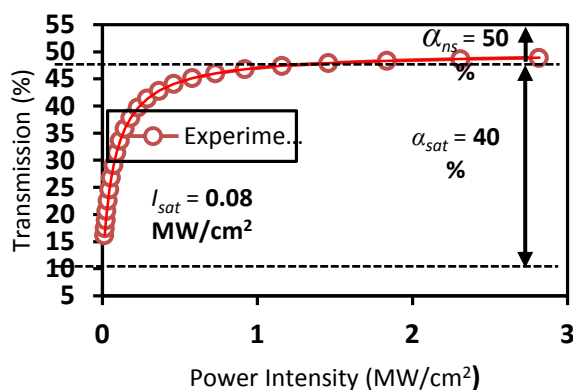


Fig. 2: Measured saturable absorption of the fabricated  $\text{TiO}_2$  film

### 3. Configuration of the $\text{TiO}_2$ based mode-locked EDFL

To evaluate the fabricated  $\text{TiO}_2$  film for mode-locking ability, the fiber laser cavity is schematically designed to operate at wavelength of  $1.5 \mu\text{m}$ . Fig. 3 shows the proposed configuration for the mode locked EDFL, which employ the fabricated  $\text{TiO}_2$  film based SA as a passive mode locker. It uses a  $1.4 \text{ m}$  long EDF, which is pumped by a  $980 \text{ nm}$  laser diode through a  $980/1550 \text{ nm}$  wavelength division multiplexer (WDM), as a gain medium. The EDF used has core and cladding diameters of  $9 \mu\text{m}$  and  $125 \mu\text{m}$  respectively, a numerical aperture of  $0.24$  and Erbium ion absorption of  $23.9 \text{ dB/m}$  at the pump wavelength of  $980 \text{ nm}$ . The  $\text{TiO}_2$  film is sandwiched between two ferrule connectors via a fiber adapter before it is inserted into the laser cavity to act as a passive mode-locker. The film has an absorption of  $3.0 \text{ dB}$  at  $1550 \text{ nm}$  region with thickness of around  $30 \mu\text{m}$ . The polarization insensitive isolator is incorporated inside the cavity to ensure unidirectional propagation of light in the laser cavity. A  $186 \text{ m}$  long single-mode fiber (SMF) was added in the cavity to gain sufficient amount of phase shift per round trip in the cavity for assisting mode-locked generation. The signal is coupled out using a  $80:20$  coupler which allows  $80\%$  of the light to oscillate in the ring cavity. The ring resonator comprises a  $1.4\text{m}$  EDF,  $186\text{m}$  of additional SMF and  $6.6\text{m}$  another SMF from the components and thus the total cavity length is approximately  $194 \text{ m}$ .

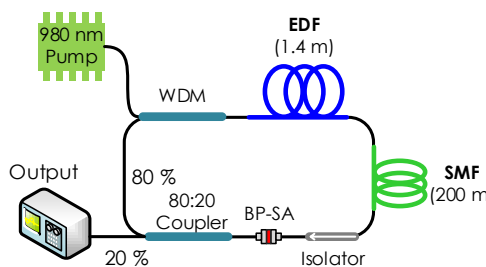


Fig. 3: The schematic setup of the mode locked EDFL employing the fabricated  $\text{TiO}_2$  film based SA.

#### 4. Mode-locking Performance

A stable self-started mode-locked pulse is generated as the pump power is increased gradually above the threshold pump power of 73 mW. This mode-locking threshold is relatively high due to by the high insertion loss of the TiO<sub>2</sub> film based SA. The TiO<sub>2</sub> film is also observed to maintain stable without thermal damage as the pump power was further increased to the maximum available pump power of 157 mW. The laser also produces a stable repetition rate, which shows that the mode-locking operation is maintained up to the maximum pump power. Fig. 4 shows the output optical spectrum measured under a pump power of 73 mW. It operates at central wavelength of 1563 nm with the 3-dB spectral bandwidth is measured to be about 0.39 nm. We also observe the optical spectrum broadening, which is most probably due to the self-phase modulation effect in the laser cavity. Fig. 5 shows the typical mode-locked pulse train at pump power of 157 mW. The repetition rate of the pulse train is obtained at 1.038 MHz, which matches with the cavity length of about 194 m. The mode-locked pulse has a pulse duration of about 271.3 ns and the time-bandwidth product is calculated to be 12987, which indicates that the optical pulse is heavily chirped. The large frequency chirp obtained verify that the generated pulse is a dissipative soliton, which its formation is a natural consequence of the mutual balance between the gain, loss, dispersion and nonlinearity characteristics inside the cavity. The formation of dissipative soliton was also widely reported in graphene based mode-locked fiber lasers [19].

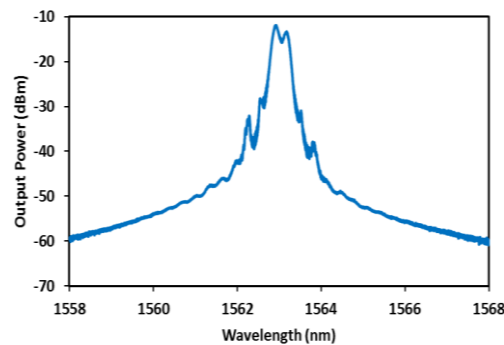


Fig. 4: Output optical spectrum at input pump power of 73 mW

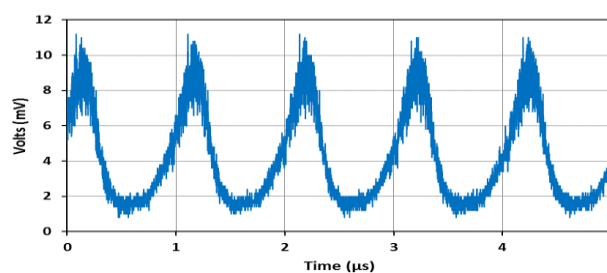


Fig. 5: Typical mode-locked pulse train at input pump power of 157 mW

Fig. 6 shows the measured average output power and the calculated single pulse energy against the input pump power. It is clearly shown that the output power increases from 3.0 mW to 6.5 mW as the corresponding pump power is tuned from threshold power of 73 mW to the maximum pump power of 157 mW. The optical-to-optical efficiency is relatively lower (4.16%) because of the high insertion loss of the SA film. On the other hand, the calculated pulse energy also almost linearly increases with the pump power. The maximum pulse energy of 6.25 nJ is obtained at the maximum pump power of 157 mW. In order to examine the stability of the laser, the radio frequency (RF) spectrum is also obtained using a RF spectrum analyzer at input pump power of 157 mW. The result is plotted in Fig. 7, which shows the

fundamental frequency of 1.038 MHz. This frequency matches to the pulse period (peak to peak duration) of the oscilloscope trace. The RF spectrum has a high SNR up to 51 dB, further indicating the stability of the obtained pulse train. Further work on reducing the film loss and optimizing the EDFL cavity is important especially for the high power operation of the laser.

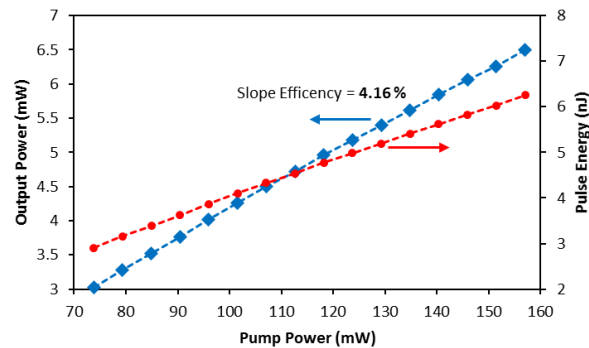


Fig. 6. Average output power and single pulse energy against the pump power.

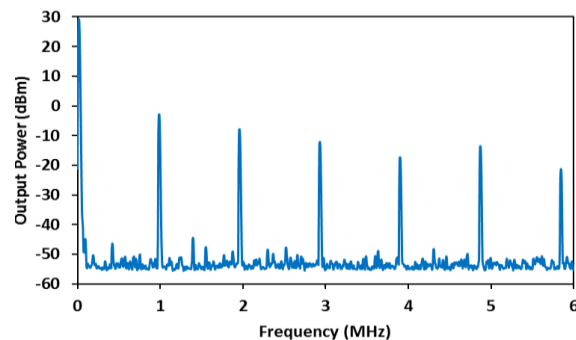


Fig. 7. The measured RF spectrum at pump power of 157 mW.

#### 4. Conclusions

Dissipative soliton mode-locked pulse trains have been successfully obtained in a ring EDFL cavity using a TiO<sub>2</sub> film as a SA. The film was prepared from precursor which was obtained by mixing the dispersed TiO<sub>2</sub> suspension into a PVA solution. It has a loss of 3.0 dB and modulation depth of 40.0% at 1550 nm. The laser operates in normal dispersion regime since a 186 m long SMF is into the ring cavity.

A stable dissipative soliton mode-locked pulse is produced as the input pump is maintained within 73 mW to the maximum power of 157 mW. The laser has a central operating wavelength, 3 dB spectral bandwidth, pulse duration, and repetition rate of 1563 nm, 0.39 nm, 271.3 ns, and 1.038 MHz, respectively. The maximum pulse energy of 6.25 nJ is achieved at the maximum input pump power of 157 mW. These results indicate that the proposed TiO<sub>2</sub> film could be useful as a simple, low-insertion-loss, low-cost, ultrafast SA device for ultrafast laser generation applications.

#### Acknowledgement

This work was financially supported by Ministry of Higher Education Grant Scheme (FRGS/1/2015/SG02/UITM/03/3) and the University of Malaya (Grant No: PG173-2015B and PG004-2016A).

## References

- [1] U. Keller, *Nature*, **424**, 831 (2013).
- [2] N. Nishizawa, *Japanese Journal of Applied Physics*, **53**, 090101 (2014).
- [3] L. Zhang, J. Zhou, Z. Wang, X. Gu, Y. Feng, *IEEE Photon. Technol. Lett.*, **26**, 1314 (2014)
- [4] A. Martinez, Z. Sun, *Nature Photon.* **7**, 842 (2013).
- [5] S. M. Azooz, S. W. Harun, H. Ahmad, A. Halder, M. C. Paul, M. Pal, S. K. Bhadra, *Chin. Phys. Lett.*, **32**, 14204 (2015).
- [6] Z. -C. Luo, M. Liu, H. Liu, X. -W. Zheng, A. -P. Luo, C. -J. Zhao, H. Zhang, S. -C. Wen, W. -C. Xu, *Opt. Lett.* **38**, 5212 (2013).
- [7] J. Du, Q. Wang, G. Jiang, C. Xu, C. Zhao, Y. Xiang, et al., *Nature scientific reports*, 4, 2014.
- [8] I. Martev, *Vacuum*, **58**, 327 (2000).
- [9] H. Elim, W. Ji, A. Yuwono, J. Xue, and J. Wang, *Appl. Phys. Lett.* **82**, 2691 (2003).
- [10] K. Iliopoulos, G. Kalogerakis, D. Vernardou, N. Katsarakis, E. Koudoumas, S. Couris, *Thin Solid Films*, **518**(4), 1174 (2009).
- [11] B. Karunagaran, K. Kim, D. Mangalaraj, J. Yi, S. Velumani, *Sol. Energy Mater. Sol. Cells*, **88**(2), 199 (2005).
- [12] "Titanium dioxide (anatase)," *Nat. Inst. Standards Technol. (NIST)*, Gaithersburg, MD, USA, 2015. [Online]. Available: <http://webbook.nist.gov/cgi/cbook.cgi?ID=C13463677&Type=IR-SPEC&Index=0-Refs>
- [13] N. Satoh, T. Nakashima, K. Kamikura, K. Yamamoto, *Nature Nanotechnol.*, **3**(2), 106 (2008).
- [14] X. Chen, *Journal of materials science letters*, **21**, 1637 (2002).
- [15] U. Balachandran, N. Eror, *Journal of Solid State Chemistry* **42**, 276 (1982).
- [16] E. Garmire, *IEEE J. Sel. Topics Quantum Electron.* **6**, 1094 (2000).
- [17] Y. Chen, C. Zhao, S. Chen, J. Du, P. Tang, G. Jiang, H. Zhang, S. Wen, D. Tang, *IEEE J. Sel. Topics Quantum Electron.*, **20**(5), 315 (2014).
- [18] H. Li, H. Xia, C. Lan, C. Li, X. Zhang, J. Li, Y. Liu, *IEEE Photon. Technol. Lett.*, **27**(1), 1041 (2015).
- [19] H. Zhang, D. Tang, R. J. Knize, L. Zhao, Q. Bao, K. P. Loh, 23. *Appl. Phys. Lett.* **96**, 111112 (2010).